Structural principles and classification of sulfosalts

By Y. Takéuchi and R. Sadanaga

Mineralogical Institute, Faculty of Science, University of Tokyo, Hongo, Tokyo

Auszug

Ein Überblick über die Dimensionen der Anionengruppe TS_3, T = As, Sb, Bi, in Sulfosalzen ergibt für die Abstände T–S bzw. S–T–S 2,26 und 2,31 Å für AsS_3, 2,46 und 2,54 Å für SbS_3 und 2,62 und 2,79 Å für BiS_3. Unter Berücksichtigung der möglichen Deformationen der Bindungswinkel werden die Abstände S–S zu 3,4–3,6 Å für AsS_3, 3,6–3,8 Å für SbS_3 und 3,8–4,1 Å für BiS_3 angenommen.

Aus den bisher bestimmten Strukturen von Sulfosalzen könnte gefolgert werden, daß das Strukturprinzip dieser Gruppe auf der räumlichen Beziehung zwischen den Koordinationspolyedern um die Metall- und die T-Atome beruht und daß die Radien dieser Atome als Maß für die Klassifikation dienen könnten. Aber die Radien, vor allem der Metallatome, lassen sich wegen der wechselnden Koordination dieser Atome nicht eindeutig angeben. Deshalb wurden statt der Atomradien versuchsweise die Hauptquantenzahlen der Valenzelektronen als Ordnungsgröße benutzt. Die Sulfosalze wurden in ein Diagramm mit dem Mittel aus den Hauptquantenzahlen $\bar{n}_A$ als Abszisse und der Summe dieser Quantenzahlen, dividiert durch die Summe der Hauptquantenzahlen der T-Atome, $\Sigma\bar{n}_A/\Sigma n_T$, eingetragen. Im Diagramm sind deutlich vier Gebiete zu erkennen, von denen ein jedes nur Strukturen eines gemeinsamen Bauschemas aufweist. Das eine Gebiet umfaßt kupferreiche Verbindungen und ist durch Verknüpfungen von CuS_4-Tetraedern allein oder mit TS_3-Pyramiden charakterisiert; das zweite hat hohen Silbergehalt und wird hauptsächlich durch die Bindungen der Silberatome bestimmt; die Strukturen des dritten Gebiets sind bleireich oder silberarm und nah verwandt mit der Bleiglanz-Struktur; das vierte Gebiet enthält Blei-Sulfosalze mit relativ hohem Gehalt an T-Atomen. Die Strukturen dieses Gebiets wurden auch in der Abhängigkeit von n_T (statt $\bar{n}_A$ als Abszisse) klassifiziert; für sie sind die Größenunterschiede zwischen den Blei-Polyedern und den TS_3-Pyramiden maßgebend.

Abstract

A survey on the dimensions of the TS_3 anionic groups in sulfosalts was carried out, where T represents a trivalent atom such as As, Sb or Bi. The average lengths of T–S non-bridge bonds and S–T–S bridge bonds are respec-

tively 2.26 Å and 2.31 for AsS_3, 2.46 and 2.54 for SbS_3 and 2.62 and 2.79 for BiS_3. After due consideration has been paid to possible deformations of bond angles, the S−S edge lengths are estimated to fall in the ranges 3.4−3.6 Å for AsS_3, 3.6−3.8 for SbS_3 and 3.8−4.1 for BiS_3.

From the structures of sulfosalts so far determined, it was concluded that the structural principle of the group is the dimensional relationship between coordination polyhedra around the metal atoms and those of T atoms, and accordingly the radii of these constituent atoms were considered to serve as effective measures for the classification. However, since the radii of metal atoms especially for various coordination states cannot be unambiguously defined, the use of the principal quantum numbers for the valence shells was proposed as a tentative measure of their atomic sizes. A diagram was then constructed of the average principal quantum number of metal atoms versus the total quantum number of the atoms divided by the total quantum number of the T atoms, and various sulfosalts were plotted in it. The diagram clearly indicated four distinct areas, each of which groups together species having a common structural scheme. The first area covers the sulfosalts containing copper in large amounts and characterized structurally by linked CuS_4 tetrahedra or by a linkage of CuS_4 and TS_3; the second covers those with high silver contents and characterized by the bonds peculiar to silver atoms; the third covers those bearing Pb in large amounts and those with low silver contents, and having close relationship to the galena structure; the fourth covers the group of lead sulfosalts having relatively high contents of T atoms.

A similar method of classification was then applied to the lead sulfosalts of the fourth area. Their structural characteristics are discussed in terms of dimensional differences between lead polyhedra and TS_3 pyramids.

Introduction

Sulfosalts comprise a group of minerals having the general formula $A_mT_nX_p$, in which the common elements are: as A: Ag, Cu, Pb; as T: As, Sb, Bi; as X: S (BERRY and MASON, 1959)[1], and they can be regarded as salts of the sulfo-acids of trivalent arsenic, antimony or bismuth. In the crystal structures of these minerals, the trivalent atom T is coordinated by three sulfur atoms to form a low pyramid, with T at the vertex and three sulfur atoms at the basal corners. Such pyramids often constitute a complex group, finite or infinite, by sharing sulfur atoms; the independent pyramids or the complex groups are linked together by monovalent atoms such as Ag and Cu or divalent atoms such as Pb or by both kinds. The presence of the TS_3 pyramids in the structure is, in fact, the feature that distinguishes a sulfosalt from a sulfide. For example, enargite might, at a glance, be thought, from its composition Cu_3AsS_4, to be a sulfosalt, but arsenic in

---

[1] BERRY and MASON have given the general formula $A_mB_nC_p$. However B is here replaced by T simply to avoid confusion with boron.

this compound is pentavalent and takes a tetrahedral coordination of sulfur atoms, thus exhibiting the aspect of a derivative from wurtzite. This species should therefore be classified as a sulfide. On the other hand, the minerals of tetrahedrite series, $Cu_{12}(As,Sb)_4S_{13}$, are often misconceived as derivatives of the sphalerite structure. However, arsenic and antimony in these minerals are trivalent and have the pyramidal coordination characteristics of sulfosalts. In fact, as pointed out by WUENSCH (1964), the crystal structure of tetrahedrite cannot be derived directly from the sphalerite structure through the substitution of Zn by Cu and (As, Sb).

In the structure of a sulfosalt the presence of anionic groups, either single or polymerized, reminds us of the structure of a silicate in which SiO_4 tetrahedra play a similar role. However, there is a difference between these two structures; the interatomic bonds in the silicate are essentially ionic, while those in sulfosalts are covalent, which means that the former are non-directional and simple, while the latter are directional and a little more complex. Certainly due to this fact, the classification of sulfosalts on the basis of their structural principles has not been established. However, since a number of important members of this group, especially those containing Cu and Pb, have been investigated and their structures have been determined at least in their main features, it is believed that we should now direct our efforts to the problem of their classification.

In the present paper, we shall begin with a general survey of the dimensions of the TS_3 group and propose principles for classification. Then we shall describe their application to the structures of sulfosalts containing Pb as the major metal atom, and discuss general structural scheme of these sulfosalts based upon the dimensional relations between TS_3 pyramids and metal polyhedra.

Dimensions of the TS₃ anionic groups

A survey of bond lengths in the structures of sulfides in general was lately carried out by BERRY (1965) and the bond lengths between trivalent atoms and sulfur atoms were also discussed. Since then, however, accurate structure determinations have been accomplished of some important members of sulfosalts, and more reliable data are now available. Therefore, it will be worthwhile revising and extending the survey. In the following, only those data from well-refined structures are employed, and bridge bonds of the S—T—S type and non-bridge

Table 1. *As—S bond lengths in sulfosalts*

	Bridge bond	Non-bridge bond		Bridge bond	Non-bridge bond
binnite[1]		2.246 Å	marrite[4]		2.259 Å
					2.269
hatchite[2]	2.35 Å	2.23			2.279
		2.23			
	2.30	2.27	proustite[5]		2.254_4
		2.25			
			rathite I[6]	2.304 Å	2.254
hutchinsonite[3]	2.31	2.30			2.237
		2.26		2.394	2.234
	2.35	2.24			2.271
	2.32			2.327	2.258
	2.33	2.25			2.251
	2.32				
	2.26 ⎫		wallisite[7]	2.34	2.28
	2.26 ⎪				2.26
	2.27 ⎬ *			2.31	2.25
	2.26 ⎪				2.27
	2.27 ⎪				
	2.27 ⎭		xanthoconite[8]		2.25
			mean	2.31	2.26

* Bond lengths in the As—S sheet configuration of hutchinsonite.

[1] Wuensch *et al.* (1966),	[2] Marumo and Nowacki (1967),
[3] Takéuchi *et al.* (1965),	[4] Wuensch and Nowacki (1967),
[5] Engel and Nowacki (1966),	[6] Marumo and Nowacki (1966),
[7] Takéuchi *et al.* (1968),	[8] Engel and Nowacki (1968).

bonds T—S will be given separate treatments because these two types of bond have revealed a marked difference in length.

Bond lengths between As and S are listed in Table 1. It will be noticed that bridge bonds are longer than non-bridge bonds. Some of the bridge bonds in hutchinsonite (Takéuchi *et al.*, 1965) are shorter than those of the rest in the table. In the structure of hutchinsonite some of the AsS_3 pyramids form a sheet by sharing every sulfur corner, and the shorter bonds are found in this sheet. The bridge bonds in orpiment, As_2S_3, whose structure is built up of a sheet of AsS_3 pyramids, also show similar values ranging from 2.21 Å to 2.28 Å (Morimoto, 1954), giving a mean value of 2.25 Å. Thus it seems certain that the bridge bonds in a sheet are shorter than the others, though the reason

Table 2. *Sb—S bond lengths in sulfosalts*

	Bridge bond	Non-bridge bond		Bridge bond	Non-bridge bond
berthierite[1]	2.58 Å	2.48 Å	livingstonite[3]	2.47 Å	2.55 Å
	2.58			2.62	
	2.48	2.43		2.59 ⎫	
	2.48			2.54 ⎪	
jamesonite[*2]	2.64	2.39		2.66 ⎬ **	
	2.49			2.52 ⎪	
	2.52	2.41		2.44 ⎪	
	2.53			2.47 ⎭	
	2.44	2.42	miargyrite[4]	2.49	2.48
	2.79			2.54	
				2.53	2.58
				2.58	
			pyrargyrite[5]		2.46$_3$
			tetrahedrite[6]		2.446
			mean	2.54	2.46

* Bond lengths were recalculated by the present authors.
** Bond lengths in the Sb—S sheet configuration of livingstonite.
[1] BUERGER and HAHN (1955),   [2] NIIZEKI and BUERGER (1957b),
[3] NIIZEKI and BUERGER (1957a),   [4] KNOWLES (1964),
[5] ENGEL and NOWACKI (1966),   [6] WUENSCH (1964).

is unknown. On the other hand, CAMERMAN and TROTTER (1964) reported that the As^{III}—S single bond in cacodyl disulfide shows a length of 2.28 Å which falls between the mean value of bridge-bond lengths and that of non-bridge bonds in Table 1. However, the sulfur atom in this compound is bonded to one more arsenic atoms in the pentavalent state and accordingly forms a bridge bond, As^{III}—S—As^{V}. The deviation from our values may therefore be due to this particular situation.

Bonds between Sb and S given in Table 2 indicate a larger difference in length between bridge bonds and non-bridge bonds than for As—S bonds. As in the case of hutchinsonite, the bridge bonds in a sheet of linked SbS_3 in livingstonite (NIIZEKI and BUERGER, 1957a) are shorter than the average.

The differences in length between bridge bonds and non-bridge bonds are still larger in sulfbismuthites. The only well-refined structure

Table 3. *Bi—S bond lengths in sulfosalts*

	Bridge bond	Non-bridge bond		Bridge bond	Non-bridge bond
galenobismutite[1]	2.79 Å	2.63 Å	cosalite[2]	2.83 Å	2.62 Å
	2.78			2.83	
	2.78			2.74	2.64
	2.73			2.74	
	2.73			2.85	2.62
				2.85	
mean	2.77	2.63		2.66	2.54
				2.66	
			mean	2.77	2.61

[1] IITAKA and NOWACKI (1962),   [2] WEITZ and HELLNER (1960).

Table 4. *Bond angles of* TS_3 *pyramids*

	S—As—S
binnite	98°22′
hatchite	98°48′ (mean)
hutchinsonite	98°12′ (mean)
marrite	98°40′ (mean)
proustite	99°24′
rathite I	98°00′ (mean of As_1, As_2 and As_3)
wallisite	98°36′ (mean)
xanthoconite	99°12′
mean*	98°39′

	S—Sb—S
berthierite**	94°00′ (mean)
livingstonite**	92°36′ (mean)
miargyrite**	94°51′ (mean)
pyrargyrite	96°20′
tetrahedrite	95°08′
mean	94°35′

	S—Bi—S	
galenobismutite**	92°0′	(mean of 81.7°, 93.4°, 95.0° and 97.3°)
cosalite**	92°0′	(mean)

* The average value of bond angles in nowackiite (MARUMO, 1967) is 101.63 ± 0.4° and it is certainly larger than others. Therefore, it was not used for calculating the mean value.

** Bond angles were calculated by the present authors.

of this group is galenobismutite (Iitaka and Nowacki, 1962), data for which are given in Table 3, together with those of the less refined structure of cosalite (Weitz and Hellner, 1960).

From the results of the above survey, we can conclude that for a certain kind of trivalent atom, the average length of bridge bonds is certainly greater than that of non-bridge bonds. Another conclusion to be drawn here is that the difference in length between bridge bonds and non-bridge bonds becomes larger with increasing atomic number of the trivalent atom, T. These facts are similar to those for the bonds
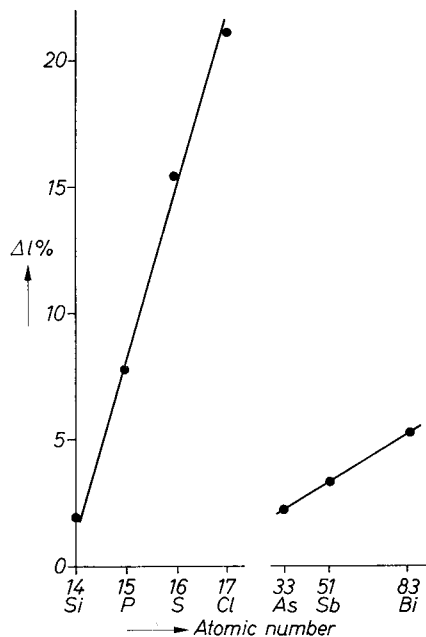
Fig. 1. Variations of the differences, Δl, between bridge bonds and non-bridge bonds in TS_3 groups (T = As, Sb, Bi), and in $(XO_4)^{n-}$ ions (X = Si, P, S, Cl)

in $(XO_4)^{n-}$ ions (X = Si, P, S or Cl) as discussed by Cruickshank (1964). A quantity Δl can be defined as (length of bridge bond—length of non-bridge bond)/(length of non-bridge bond). The average value of Δl for each T—S (T = As, Sb, Bi) was evaluated and plotted in Fig. 1 together with that of each X—O [2]. As observed in this figure Δl of the T—S bonds shows a linear variation with atomic number similar to that of $(XO_4)^{n-}$ ions.

---

[2] Calculated from the data appearing in Cruickshank (1964).

Because of the p-orbital nature of the bonds in TS_3 groups, the bond angles are expected to approach $90°$ as the bond lengths between T and S increase. As seen in Table 4, this relation does hold for the TS_3 groups. Thus, as reasonable measures for dimensions of the TS_3 groups, the following values may be proposed:

		AsS_3	SbS_3	BiS_3
Bond length	bridge	2.31 Å	2.54 Å	2.79 Å
	non-bridge	2.26 Å	2.46 Å	2.62 Å
Bond angle		98.8°	94.6°	92.0°

Next, we shall refer to S—S edge lengths in the TS_3 groups where we must take possible deformation of bond angles into account. If two pyramids share an edge, the bond angles concerned will become smaller, while if a pyramid shares an edge with a coordination polyhedron (around lead for example) the bond angle concerned will become larger. After due consideration has been paid to these circumstances, the S—S edge lenths are estimated to fall in the ranges: 3.4—3.6 Å for AsS_3, 3.6 —3.8Å for SbS_3, and 3.8—4.1 Å for BiS_3.

So far we have taken into account the three shortest distances between T and S in the TS_3 group with the assumption that the bonds involved are solely of p-orbital character. However, the facts revealed by the crystal structure of stibnite, Sb_2S_3, should also be considered. According to ŠĆAVNIČAR (1960), the structure contains a ribbon-like configuration with the composition Sb_4S_6. Two kinds of Sb atoms, Sb(1) and Sb(2), exist in a ribbon. Sb(1) is surrounded by three sulfur atoms and Sb(2) by five. Therefore, the bonds for Sb(1) are presumably of p character, the Sb—S distances being 2.58 Å for bridge bonds and 2.57 Å for non-bridge ones and the mean bond angle, 91.43°. For Sb(2), ŠĆAVNIČAR assumed octahedral sp^3d^2 orbitals in which a pair of electrons forms a lone pair. The five sulfur atoms thus constitute a square pyramid with an antimony atom situated roughly at the centre of the basal square. The distances from Sb(2) to two basal sulfur atoms are 2.68 Å; to the other two basal atoms 2.82 Å; and to the apical atom 2.49 Å; and the mean bond angle is 89.19°. This fact suggests that some of the T—S bonds in sulfosalts may also be of octahedral character. As a matter of fact, five coordination around antimony can be noticed in the structure of berthierite, $FeSb_2S_4$ (BUERGER and HAHN, 1955) and livingstonite, $HgSb_4S_8$ (NIIZEKI and BUERGER, 1957a), though three sulfur atoms of the five are appreciably nearer to anti-

mony than those in the case of stibnite. If the octahedral orbitals are involved in T—S bonds, the T atom is expected to be surrounded by seven sulfur atoms as shown in Fig. 2, because repulsion arises between the lone-pair electrons and the sulfur atoms, and in fact, those antimony atoms in stibnite, berthierite and livingstonite have seven neighbouring sulfur atoms.
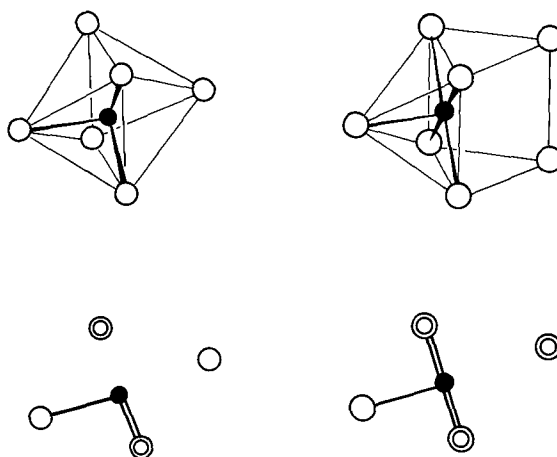

Fig. 2. Octahedral neighbours of a TS_3 group which utilizes p^3 orbitals (left), and seven neighbours of sulfur atoms around a T atom which utilizes sp^3d^2 orbitals (right). The lower figures indicate the projections of each polygon along its vertical edges

On the other hand, in addition to p^3 orbitals, tetrahedral sp^3 orbitals are also possible in certain sulfosalts. The bond angles of SbS_3 pyramids in chalcostibite, $CuSbS_2$ (Hofmann, 1933), suggest that the bonds are of tetrahedral character, where a pair of electrons forms a lone pair.

Classification of sulfosalts

In order to classify the sulfosalts, we must first establish what principles govern the general relationship between the chemical compositions and the crystal structures of this group of minerals. As far as our survey of all the refined structures is concerned, we believe that the principle determining the structure is the dimensional relationship between the coordination polyhedra around monovalent and divalent metal atoms which we shall call 'A atoms' hereafter, and those around trivalent atoms which we shall call 'T atoms'. Accordingly, the radii of

these constituent atoms can be considered as effective parameters for the classification. This will be exemplified in the subsequent section on the structures of the Pb-bearing members.

On the other hand, however, the radii of these atoms for various coordination states cannot unambiguously be determined. Therefore, we here propose as tentative measures of their atomic sizes the principal quantum numbers of the valence shells of these atoms.

Since there are a number of sulfosalts which contain two, or more than two, kinds of A atoms, we introduce the 'average principal quantum number', $\bar{n}(A)$, defined as

$$\bar{n}(A) = \Sigma\, k_i \cdot n(A_i)/\Sigma k_i ,$$

where $n(A_i)$ is the principal quantum number for the valence shell of an A atom of the kind i, and k_i is the number of the atoms per formula unit. The quantity, $\bar{n}(A)$, will thus be a measure of the average size of A atoms existing in a structure. This parameter will also be used as a measure of the directional character of metal atoms involved in a structure (PEARSON, 1964).

Next, we take a ratio, $\Sigma\, n(A_i)/\Sigma\, n(T_j)$, where $n(T_j)$ indicates the principal quantum number for the valence shell of a T atom of the kind j, and summations should be made for the formula unit. This ratio is intended to serve as an indication of the volume occupied by A atoms relative to that occupied by T atoms in the structure under consideration. A diagram of $\bar{n}(A)$ vs. $\Sigma\, n(A_i)/\Sigma\, n(T_j)$ was then prepared and the natural crystalline phases of sulfosalts were plotted (Fig. 3). As will be observed, this diagram is roughly divided into four parts according to the structural characteristics of the crystalline phases.

Area I covers the sulfosalts which contain copper as a major component. The crystal structures of sulfosalts which fall in this area are thus characterized by the linkages of Cu tetrahedra (e.g. tetrahedrite) or those of Cu tetrahedra and TS_3 pyramids (e.g. chalcostibite). At the right of this area, there is located a group of sulfosalts—seligmannite, $PbCuAsS_3$; bournonite, $PbCuSbS_3$, and aikinite, $PbCuBiS_3$. HELLNER and LEINEWEBER (1956) showed that they have similar structures and pointed out the similarity between their structures and that of stibnite. However, TAKÉUCHI and HAGA (1969) refined the atomic parameters of seligmannite using the structure amplitudes given by LEINEWEBER (1956), and proposed a new view that it is essentially built up of a three-dimensional framework consisting of CuS_4 tetrahedra and AsS_3
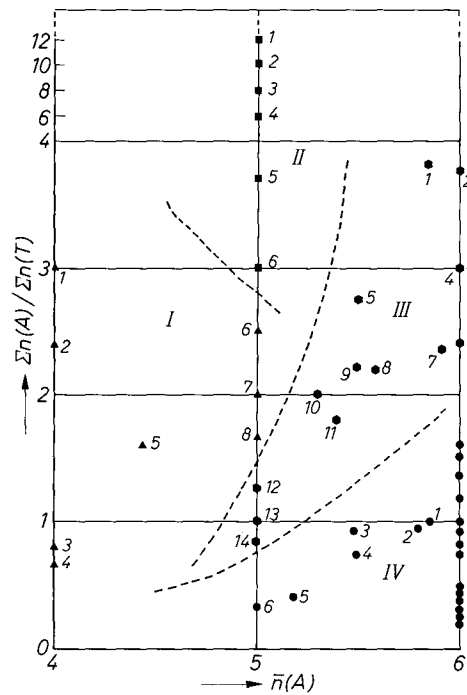
Fig. 3. The relations between the chemical compositions and the crystal structures of sulfosalts. Representative minerals in each area are:

Area I

1 binnite, $(Cu,Fe)_{12}As_4S_{13}$
2 tetrahedrite, $(Cu,Fe)_{12}Sb_4S_{13}$
3 chalcostibite, $CuSbS_2$
4 emplectite, $CuBiS_2$
5 berthonite, $Pb_2Cu_7Sb_5S_{13}$
6 seligmannite, $PbCuAsS_3$
7 bournonite, $PbCuSbS_3$
8 aikinite, $PbCuBiS_2$

Area II

1 polyargyrite, $Ag_{24}Sb_2S_{15}$?
2 pearceite, $(Ag,Cu)_{16}As_2S_{11}$
3 polybasite, $(Ag,Cu)_{16}Sb_2S_{11}$
4 stephanite, Ag_5SbS_4
5 xanthoconite, Ag_3AsS_3
6 pyrargyrite, Ag_3SbS_3

Area III

1 lengenbachite, $Pb_{36}Ag_7Cu_6As_{23}S_{78}$
2 gratonite, $Pb_9As_4S_{15}$

3 geocronite, $Pb_5(Sb,As)_2S_8$
4 beegerite, $Pb_6Bi_2S_9$
5 marrite, $PbAgAsS_3$
6 jordanite, $Pb_{13}As_7S_{23}$
7 meneghinite, $Pb_{13}CuSb_7S_{23}$
8 hatchite, $TlPbAgAs_2S_5$
9 freieslebenite, $PbAgSbS_3$
10 wallisite, $TlPbCuAs_2S_5$
11 diaphorite, $Pb_2Ag_3Sb_3S_8$
12 smithite, $AgAsS_2$
13 miargyrite, $AgSbS_2$
14 matildite, $AgBiS_2$

Area IV

1 ramdohrite, $Pb_3Ag_2Sb_6S_{13}$
2 fizelyite, $Pb_5Ag_2Sb_8S_{18}$
3 jamesonite, $FePb_4Sb_6S_{14}$
4 andorite, $PbAgSb_3S_6$
5 rezbanyite, $Pb_3Cu_2Bi_{10}S_{19}$
6 gladite, $PbCuBi_5S_9$

Details of the mineral species on the vertical axis of $\bar{n}$ (A) = 6 in the area IV are described in Fig. 7

pyramids, lead atoms being inserted in the large spaces in the frame-work. In general, in the crystal structures of sulfosalts of this area the linkages of Cu tetrahedra, or those of Cu tetrahedra and TS_3 pyramids, are closely related to the simple tetrahedral structures observed in sulfides.

Area II covers the silver sulfosalts containing more silver. Although only the crystal structures of pyrargyrite, Ag_3SbS_3 (HARKER, 1936; ENGEL and NOWACKI, 1966), and xanthoconite, Ag_3AsS_3 (ENGEL and
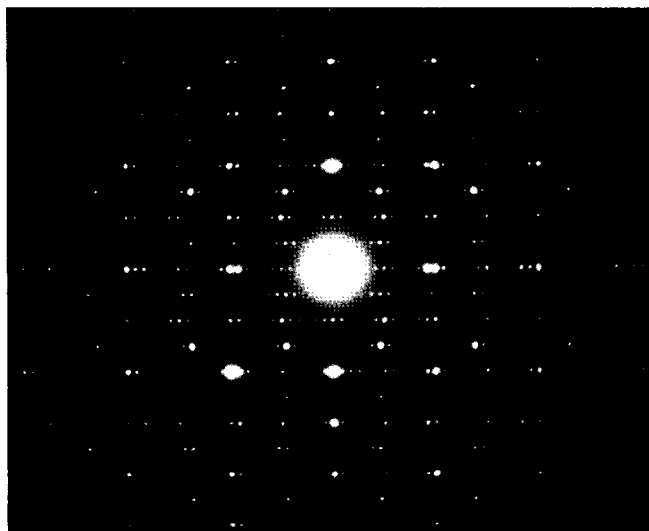

Fig. 4. An electron-diffraction pattern of lengenbachite showing $hk0$ reflections (taken by S. SUENO). The regular arrangement of stronger reflections indicates the subcell of the galena type

NOWACKI, 1968), are known, the crystal structures of these sulfosalts are characterized by covalent bonds which are specific to the silver atoms.

The minerals which fall in the area III, which extends from the central part to the diagram upper to the right, are indicated by solid hexagons. Most of these sulfosalts were investigated by x-ray methods and it has been found that their structures are closely related to the galena-type structure. Matildite, $AgBiS_2$ (GELLER and WERNICK, 1959), miargyrite, $AgSbS_2$ (KNOWLES, 1964), freieslebenite, $PbAgSbS_3$ (HELL-NER, 1957) and diaphorite, $Pb_2Ag_3Sb_3S_8$ (HELLNER, 1958) are typical examples. They all are based upon the PbS-type structure, and in fact

they transform to disordered PbS-type structures at an elevated temperature (Wernick, 1960). Although in the crystal structure of wallisite (Takéuchi et al., 1968), which contains copper as a major component, the copper tetrahedra and AsS_3 pyramids form a composite chain, the arrangements of lead and sulfur atoms are closely related to the galena structure. Some other minerals in this area, like lengenbachite, $Pb_{36}Ag_7Cu_6As_{23}S_{78}$, and franckeite, $Pb_5Sn_3Sb_2S_{14}$, give diffraction patterns which are characterized by a marked subcell of the galena type (Fig. 4), suggesting that, in spite of the complexity of the chemical compositions, the structures are based upon that of galena.

The final area IV, which extends from the lower right part of the diagram to the left, covers the great majority of the lead sulfosalts. Since these are relatively rich in trivalent atoms, they show, in contrast to the singular aspect common to the lead sulfosalts in the area III, various structures depending upon the Pb-to-T atom ratio. If the ratio is higher, the structures are characterized by the linkage of lead polyhedra while, if the ratio is lower, they are characterized by those of the pyramids of T atoms. Therefore their structures are primarily to be interpreted in terms of the dimensional differences between lead polyhedra and T pyramids. Thus, from the structural view point, they are the most interesting subgroup of sulfosalts, and the variation of their structures with chemical compositions is discussed below, in terms of the above-mentioned dimensional differences.

With this diagram (Fig. 3) the basic principles of the crystal structure of a given sulfosalt could be predicted, provided that its chemical composition were known. However, this diagram seems to be less applicable to sulfosalts which contain transitional elements as metal atoms. For instance, samsonite, $MnAg_4Sb_2S_6$ for which $\bar{n}(A) = 4.8$, $\Sigma n(A)/\Sigma n(T) = 2.4$, falls in the area I, but it is not likely that the structure is characterized by a tetrahedral linkage of metal atoms.

General characteristics of lead sulfosalts

The most common coordination of lead in sulfides is octahedral, as occurs in galena, the Pb—S distance being 2.965 Å (Swanson and Fuyat, 1953). This bond length in galena implies that the edges of the octahedra are 4.19 Å long, provided that the octahedra are of regular shape. This value is longer than the edges in any TS_3 pyramids. Therefore sharing edges between octahedra and pyramids inevitably gives rise to a deformation of these polyhedra. Since bonds in pyramids are stronger than those in octahedra, it is expected that the deformations

are much more conspicuous for octahedra. Greater deformations are evidently to be expected if the lead octahedra share edges with AsS_3 pyramids, the smallest. For this case, as shown in Fig. 5, the deformations in octahedra produce a fairly large open space which allows further sulfur atoms to approach the central lead atom, thus increasing
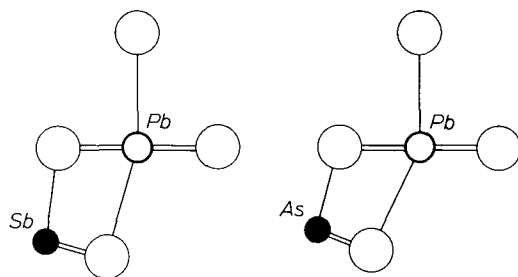

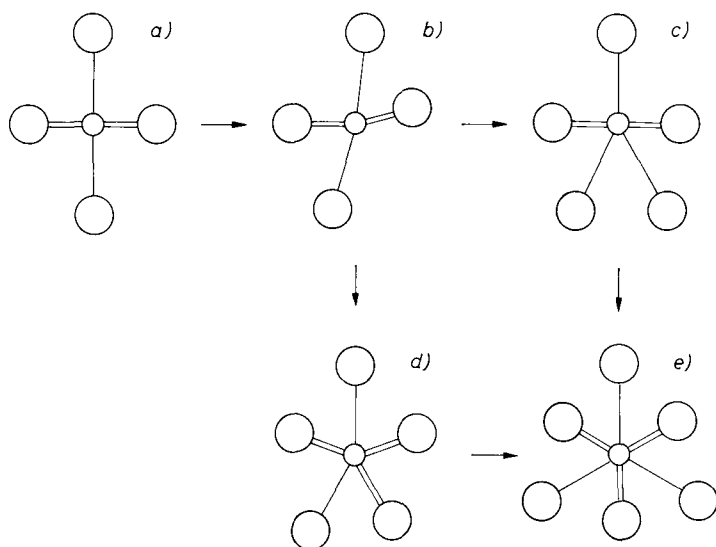Fig. 5. Deformations of a Pb-S octahedron caused by sharing an edge with an SbS_3 pyramid (left), and with an AsS_3 pyramid (right)

Fig. 6. A regular Pb-S octahedron (a) may be deformed (b) if it shares an edge with a certain TS_3 group, producing an open space which allows further sulfur atoms to approach the lead atom. If one sulfur atom approaches, a lead polyhedron of coordination number seven results (c); if two approach, that of coordination number eight is obtained (d). Further deformations of the Pb-S polyhedron by sharing edges with TS_3 groups finally yield the polyhedron of nine-fold coordination (e)

the coordination of lead. In fact, in most of the lead sulfarsenites, lead atoms have coordination number nine, which is the highest so far observed for lead. Six of the nine sulfur atoms in such lead polyhedra form, as illustrated in Fig. 6, a trigonal prism whose edges are of lenghts similar to those in lead octahedra and each of the other three sulfur atoms forms a square pyramid on each prism face.

Since SbS_3 and BiS_3 pyramids cause relatively less distortion of lead octahedra, the lead polyhedra in the structure of sulfantimonites and sulfbismuthites generally take a form intermediate between octahedra and the nine-coordinated polyhedra just mentioned. They may also be distorted octahedra (Fig. 6). The coordination number of lead in these sulfosalts is therefore 6, 7, 8. The ratio between the number of octahedra and the number of intermediate polyhedra in a structure depends on the content of lead relative to that of the T atoms.

These relations among the lead sulfosalts can be systematized if we apply the principle discussed in the preceeding section. Using it, we can further classify the lead sulfosalts. We then introduce two parameters: the first is the principal quantum number of the trivalent atoms, $n(T)$, and the other is $\sum n(A_i)/\sum n(T_j)$ just as the diagram of Fig. 3. Figure 7 is then a diagram in which the second parameter is plotted along the vertical axis and the first along the horizontal. On the left of this diagram there appear only sulfarsenites, in the middle sulfantimonites and on the right sulfbismuthites. The area of this diagram can be roughly divided into three parts according to types of lead polyhedra occurring in the structures.

In the structures of sulfosalts in the upper right area of this diagram, both octahedra and intermediate polyhedra occur, and in those of the central area, only intermediate types. In those of the left part, which covers the sulfarsenites, the nine-fold coordination appears. Among sulfarsenites, hutchinsonite (Takéuchi et al., 1965) which is most rich in arsenic, is somewhat exceptional. Since half of the arsenic atoms of hutchinsonite form a sheet structure, the number of arsenic atoms surrounding lead-sulfur polyhedra is less than in other sulfarsenites. Thus only intermediate polyhedra of lead occur in its structure. With this exception of hutchinsonite, we can observe that, in this diagram, the coordination number of lead increases from the upper right to the lower left.

Such a general tendency in the structures of lead sulfosalts can be explained as follows: As already discussed, bismuth and antimony may have coordination polyhedra which simulate distorted octahedra,

though bonding is only with the three closest neighbors. These distorted octahedra tend to form, together with lead octahedra, a fragment of the galena-type structure. If the ratio of $\Sigma n(\text{A})$ to $\Sigma n(\text{T})$ is
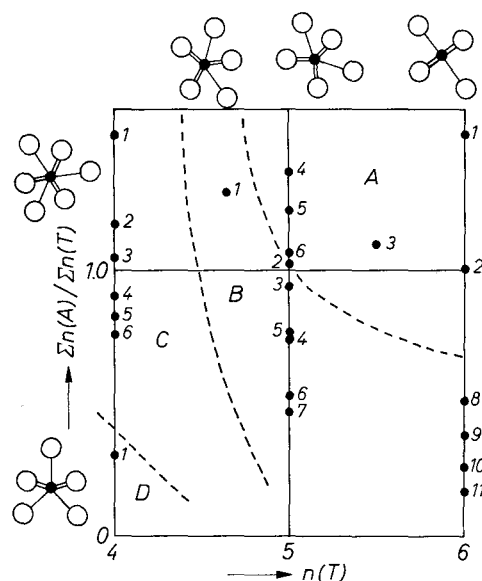

Fig. 7. Relations between chemical compositions and types of lead polyhedra of sulfosalts in the area IV (Fig. 3). Representative minerals are explained below. Since each chemical formula has a general form, $\text{Pb}_m\text{T}_n\text{S}_p$, it is given in an abbreviated form, $m\ n\ p$. Those which have not the general form are given in full.

Area A

1 lillianite*, 3 2 6
2 cosalite, 2 2 5
3 kobellite*, 2 2 5
4 semseyite*, 9 8 21
5 boulangerite, 2 2 5
6 heteromorphite*, 7 8 19

Area B

1 veenite*, 2 2 5
2 fizelyite**
3 jamesonite**
4 andorite**
5 plagionite*, 5 8 17
6 zinkenite, 6 14 27
7 fuloppite*, 3 8 15

* Unknown structure.

8 galenobismutite, 1 2 4
9 chiviatite*, 3 8 15
10 bonchevite*, 1 4 7
11 ustrasite*, 1 6 10

Area C

1 dufrenoysite, 4 4 10
2 rathite-Ia, 7 9 20
3 rathite-II, 9 13 28
4 rathite-I, 3 5 10
5 baumhauerite, 5 9 18
6 scleroclase, 2 4 8

Area D

1 hutchinsonite, $\text{PbTlAs}_5\text{S}_9$

** Chemical formula is given in Fig. 3.

large, the distortions in the fragments may be accomodated locally and the whole structure is of the galena type. On the other hand, if the ratio becomes smaller, the distortions in fragments increase and the extent of the fragments is limited. Therefore, they join in various ways to form a structure. In the boundaries between these fragments, the intermediate type of lead polyhedra occurs (Fig. 8). The occurrence of these intermediate polyhedra (which are not octahedra) presumably plays a role in minimizing the distortions accumulated when the frag-
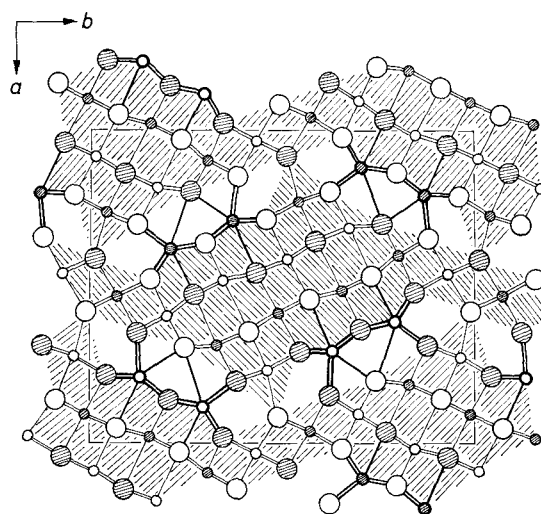
Fig. 8. The crystal structure of cosalite projected along the c axis, showing the fragments of the galena-type structure (shaded area). The bonds of intermediate Pb-S polyhedra are indicated by heavy lines. Large circles are sulfur atoms, and small ones in the shaded area are lead or bismuth. The shaded circles and open circles are respectively at $z = 3/4$ and $z = 1/4$ [after Weitz and Hellner (1960), but with some changes]

ments are joined. This is the case of sulfosalts in the upper right area of the diagram. Now, as the ratio decreases further, the fragments come to consist solely of trivalent atoms, and the lead atoms occur only in the boundaries of these fragments. This is the case of sulfosalts in the central area of the diagram. Since the pyramids of arsenic atoms have the smallest dimensions, they no longer form structural fragments of the galena type in the structures of sulfarsenites of the left part of the diagram, and lead octahedra are generally highly deformed to have the nine-fold coordination.

Next, we discuss in a different way the effects of the dimensional differences between pyramids and lead polyhedra. In the structure of lead sulfosalts, the nine-coordinated polyhedra tend to share basal triangles to form an infinite chain, while octahedra share edges and also form an infinite chain (Fig. 9). Since both chains have repeat distances of about 4.19 Å, the great majority of lead sulfosalts have cell edges of about 4.19 Å or its multiples. Without exception the single repeat distance appears in sulfbismuthites. This is because the BiS_3
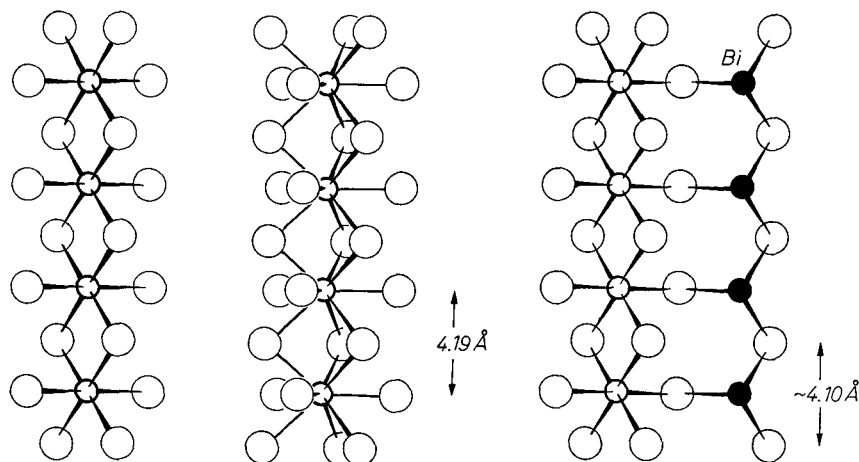
Fig. 9   Fig. 10

Fig. 9. Infinite chains of Pb-S octahedra (left), and of nine-fold polyhedra (right)

Fig. 10. A chain of BiS_3 pyramids along that of Pb-S octahedra

pyramids are the largest and their edge lengths are very close to those of lead octahedra. Therefore BiS_3 pyramids may share corners and form an infinite chain whose repeat distance is in conformity with that of lead chain. Figure 10 shows the general scheme of how the lead chains and BiS_3 chains are connected together. It should be noted that, in sulfbismuthites, the repeat distances along the chain directions are around 4.10 Å and less than the ideal repeat distance of the lead chains. Therefore, the slightly smaller repeat distance of the BiS_3 chains presumably causes the shrinkage of lead chains along their lengths.

On the contrary, the single repeat distance never occurs in sulf-arsenites but the repeat distances are generally multiple of just about 4.19 Å, the ideal value. This is explicable in that the edges of AsS_3

pyramids are much smaller than those of the lead polyhedra and, thus, for this case of sulfarsenites the formation of infinite chains like BiS_3 is not possible but the AsS_3 pyrmids form various finite chains along the chain direction of lead polyhedra as given in Fig. 11. The arrangement of these finite chains along lead chains determines the repeat distance of a structure along the direction of the lead chains, and therefore, the single repeat distance of the lead chains is no longer the true repeat distance in this direction. Since it is conceivable that such a mode of arrangement of finite chains minimizes the deformation of lead chains
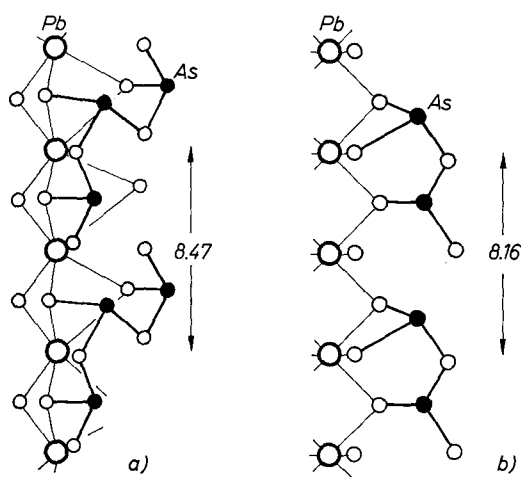

Fig. 11. Finite chains or groups of AsS_3 pyramids along Pb-S chains. (a) rathite-I, (b) hutchinsonite

along their lengths, the repeat distance of lead chains may retain their ideal value 4.19 Å. In this way, it is understandable why the repeat distances of sulfarsenites along the chain direction are multiples of the ideal 4.19 Å. The repeat distances or sub-repeat distances along chain directions are compared for sulfbismuthites, sulfantimonites and sulfarsenites in Fig. 12.

The dimensions of SbS_3 pyramids are in between those found in the above two cases and, as observed in Fig. 12, the repeat distances along lead chains do not show a characteristic value as do other cases, but are distributed over a wide range. We can observe, in fact, various types of SbS_3 linkages in sulfantimonites. They may be divided into three categories. Firstly, along lead chains SbS_3 pyramids form single infinite

chains like BiS_3. Such a configuration of pyramids appears especially in the structures which contain smaller metal atoms like Fe in addition to lead. Thus this type of chain is observed in berthierite, $FeSb_2S_4$ (BUERGER and HAHN, 1955), and jamesonite, $FePb_4Sb_6S_4$ (NIIZEKI and BUERGER, 1957b). For these cases, if lead is present, the Pb-S chain is
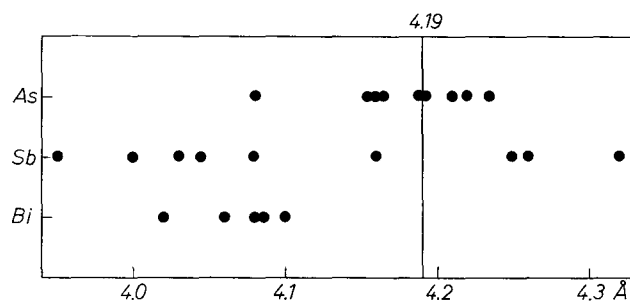

Fig. 12. Comparison of the repeat distances or sub-repeat distances along Pb-S chain directions of various sulfarsenites (As), sulfantimonites (Sb), and sulfbismuthites (Bi) in the area IV (Fig. 3)
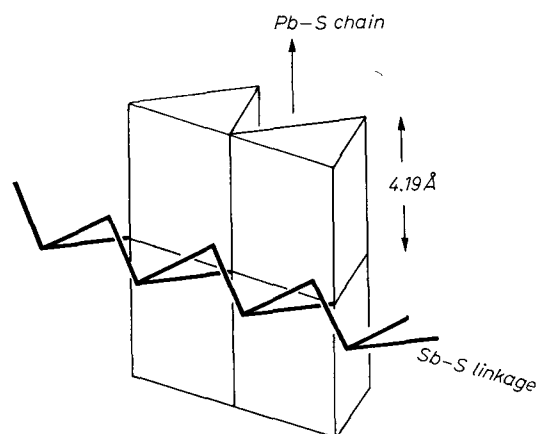

Fig. 13. A schematic illustration of the lateral linkage of SbS_3 pyramids with respect to Pb-S chains in jamesonite

subject to contraction along the chain direction and shows a smaller repeat distance than 4.19 Å. For example, the repeat distance of jamesonite along chain direction is 4.03 Å. Secondarily, the pyramids form a complex chain so as to minimize the deformation of Pb-S chains. An example of such a chain has been reported for livingstonite,

$HgSb_4S_8$ (Niizeki and Buerger, 1957a). Finally, the pyramids form a lateral linkage with respect to lead chains, as two of the three non-equivalent Sb in jamesonite (Fig. 13). These various possible linkages of SbS_3 pyramids may account for the various repeat distances of sulf-antimonites along lead chains.

In addition to the lead sulfosalts so far discussed, there are, in area IV of the diagram (Fig. 3), a few sulfosalts which contain thallium atoms as A atoms like lorandite, $TlAsS_2$, and vrbaite, $TlAs_2SbS_5$. However, owing to the fact that thallium atoms tend to form a polyhedron of sulfur atoms which is different from lead-sulfur polyhedra as observed in lorandite (Zemann and Zemann, 1959), a slight modification of the above discussions would be necessary to extend them to the sulfosalts whose A atoms are solely thallium.

Added in proof: After this paper was sent for publication, Professor Menzer kindly pointed out us a Nowacki's paper presented at the meeting of crystallographers at Bern, October 1968, whose abstract was later published in this journal, Vol. **128** (1969) 427–428 and full paper in Schweizer Mineralogisch-Petrographische Mitteilungen, Vol. **49** (1969) 109–156 under the title ,,Zur Klassifikation und Kristallchemie der Sulfosalze". In this paper, Nowacki mainly discussed the configurations of anionic groups consisting of TS_3 pyramids in terms of φ value, the ratio of the number of S atoms to that of T atoms in a formula unit. He then showed that possible topological features of the anionic groups are deduced from a given φ value.

In connection with our paper, we should also mention a work done by E. Hellner [A structural scheme for sulfide minerals. J. Geol. **66** (1958) 503–525], in which he successfully systematized the structures of sulfides and sulfosalts on the basis of the closest-packings of sulfur atoms. After his work was published, a number of detailed structures have become available, giving an information on the distortions of sulfur lattices mainly due to the formation of TS_3 pyramids characteristic of sulfosalts. Since distortion of a structure is an important aspect in crystal chemistry, we placed much stress upon this point.

References

L. G. Berry (1965), Recent advances in sulfide mineralogy. Amer. Min. **50**, 301–313.

L. G. Berry and Brian Mason (1959), *Mineralogy*. W. H. Freeman and Co., San Francisco.

M. J. Buerger and Theodor Hahn (1955), The crystal structure of berthierite, $FeSb_2S_4$. Amer. Min. **40**, 226–238.

N. Camerman and J. Trotter (1964), Stereochemistry of arsenic, Part XI. "Cacodyl disulphide", dimethylarsino dimethyldithioarsinate. J. Chem. Soc. [London] 219—227.

D. W. J. Cruickshank (1964), The rôle of $3d$ orbitals in π bonds between (a) silicon, phosphorus, sulphur, or chlorine and (b) oxygen or nitrogen. J. Chem. Soc. 5486—5504.

P. Engel und W. Nowacki (1966), Die Verfeinerung der Kristallstruktur von Proustit, Ag_3AsS_3, und Pyrargyrit, Ag_3SbS_3. N. Jahrb. Miner. Monatsh. 181—184.

P. Engel und W. Nowacki (1968), Die Kristallstruktur von Xanthokon, Ag_3AsS_3. Acta Crystallogr. B24, 77—80.

S. Geller and J. H. Wernick (1959), Ternary semiconducting compounds with sodium chloride structure: $AgSbSe_2$, $AgSbTe_2$, $AgBiS_2$, $AgBiSe_2$. Acta Crystallogr. 12, 46—54.

D. Harker (1936), The application of the three-dimensional Patterson method and crystal structures of proustite, Ag_3AsS_3, and pyrargyrite, Ag_3SbS_3. J. Chem. Physics 4, 281—390.

Erwin Hellner (1957), Über komplex zusammengesetzte sulfidische Erze, II. Zur Struktur des Freieslebenit, $PbAgSbS_3$. Z. Kristallogr. 109, 284—295.

Erwin Hellner (1958), Über komplex zusammengesetzte Spießglanze, III. Zur Struktur des Diaphorits, $Ag_3Pb_2Sb_3S_8$. Z. Kristallogr. 110, 169—174.

E. Hellner und G. Leineweber (1956), Über komplex zusammengesetzte sulfidische Erze. I. Zur Struktur des Bournonits, $CuPbSbS_3$, und Seligmannits, $CuPbAsS_3$. Z. Kristallogr. 107, 150—154.

W. Hofmann (1933), Strukturelle und morphologische Zusammenhänge bei Erzen vom Formeltypus ABC_2. I. Die Struktur von Wolfsbergit $CuSbS_2$ und Emplektit $CuBiS_2$ und deren Beziehung zu der Struktur von Antimonit Sb_2S_3. Z. Kristallogr. 84, 177—203.

Y. Iitaka and W. Nowacki (1962), A redetermination of the crystal structure of galenobismutite, $PbBi_2S_4$. Acta Crystallogr. 15, 691—698.

Charles R. Knowles (1964), A redetermination of the structure of miargyrite, $AgSbS_2$. Acta Crystallogr. 17, 847—851.

G. Leineweber (1956), Struktur-Analyse des Bournonits und Seligmannits mit Hilfe der Superpositions-Methoden. Z. Kristallogr. 108, 161—184.

F. Marumo (1967), The crystal structure of nowackiite, $Cu_6Zn_3As_4S_{12}$. Z. Kristallogr. 124, 352—368.

F. Marumo and W. Nowacki (1966), The crystal structure of rathite-I. Z. Kristallogr. 122, 433—456.

F. Marumo and W. Nowacki (1967), The crystal structure of hatchite, $PbTlAgAs_2S_5$. Z. Kristallogr. 125, 249—265.

N. Morimoto (1954), The crystal structure of orpiment, As_2S_3, refined. Mineral. Journ. 1, 160—169.

N. Niizeki and M. J. Buerger (1957a), The crystal structure of livingstonite, $HgSb_4S_8$. Z. Kristallogr. 109, 129—157.

N. Niizeki and M. J. Buerger (1957b), The crystal structure of jamesonite, $FePb_4Sb_6S_{16}$. Z. Kristallogr. 109, 161—183.

W. B. Pearson (1964), The crystal structures of semiconductors and general valence rule. Acta Crystallogr. 17, 1—15.

S. Ščavničar (1960), The crystal structure of stibnite, A redetermination of atomic positions. Z. Kristallogr. **114**, 85—97.

H. E. Swanson and R. R. Fuyat (1953), NBS Circular 539, **II**, 18.

Y. Takéuchi, S. Ghose and W. Nowacki (1965), The crystal structure of hutchinsonite, $(Tl, Pb)_2As_5S_9$. Z. Kristallogr. **121**, 321—348.

Y. Takéuchi and N. Haga (1969), On the crystal structures of seligmannite, $PbCuAsS_3$, and related minerals. Z. Kristallogr. **130**, 254—260.

Y. Takéuchi, M. Ohmasa and W. Nowacki (1968), The crystal structure of wallisite, $PbTlCuAs_2S_5$, the Cu analogue of hatchite, $PbTlAgAs_2S_5$. Z. Kristallogr. **127**, 349—365.

G. Weitz und E. Hellner (1960), Über komplex zusammengesetzte sulfidische Erze. VII. Zur Kristallstruktur des cosalits, $Pb_2Bi_2S_5$. Z. Kristallogr. **113**, 385—402.

J. H. Wernick (1960), Constitution of the $AgSbS_2$—PbS, $AgBiS_2$—PbS, and $AgBiS_2$—$AgBiSe_2$ systems. Amer. Min. **45**, 591—598.

Bernhardt J. Wuensch (1964), The crystal structure of tetrahedrite, $Cu_{12}Sb_4S_{13}$. Z. Kristallogr. **119**, 437—453.

B. J. Wuensch and W. Nowacki (1967), The crystal structure of marrite, $PbAgAsS_3$. Z. Kristallogr. **125**, 459—488.

B. J. Wuensch, Y. Takéuchi and W. Nowacki (1966), Refinement of the crystal structure of binnite, $Cu_{12}As_4S_{13}$. Z. Kristallogr. **123**, 1—20.

A. Zemann and J. Zemann (1959), Zur Kenntnis der Kristallstruktur von Lorandit, $TlAsS_2$. Acta Crystallogr. **12**, 1002—1006.